

Improved Parameterization of an Ethylene Carbonate Molecular Dynamics Model in Li-Air Batteries for Accurate Density and Transition Temperatures

D. K. Ward^a, R. E. Jones^b, J.A. Templeton^c, K.R. Reyes^d, and M. Kane^d

^a Radiation and Nuclear Detection Materials and Analysis Department, Sandia National Laboratories, Livermore, California 94550, USA

^b Mechanics of Materials Department, Sandia National Laboratories, California 94550, USA

^c Thermal/Fluid Science and Engineering Department, Sandia National Laboratories, Livermore, California 94550, USA

^d Materials Chemistry Department, Sandia National Laboratories, Livermore, California 94550, USA

(150 words)

Li-air batteries are at the forefront of advanced battery technologies because of their tremendous theoretical energy density. However, before reaching this potential several technical issues must be understood including optimal electrolytes for Li⁺ transport. With a vast library of potential electrolytes it is highly impractical to test all materials. Fortunately, atomistic models can assist in selecting optimal electrolyte candidates and thus decrease experimental time. In order for such models to effectively screen electrolyte materials, an interatomic potential must accurately reproduce relevant material properties such as density, viscosity, and transition temperatures. This work presents an approach to calibrate molecular dynamics models to capture these quantities. As a case study we explore the ability of an interatomic potential to correctly predict the transition temperature of ethylene-propylene carbonate mixtures. Here, we modify an available CHARMM potential parameterization to correctly reproduce the relative transition temperatures by modifying the long-range interactions between molecules. In doing this, we can improve the predicted transport properties of carbonate electrolytes which affect battery performance.

Introduction

Li-air batteries have the potential to provide unprecedented gravimetric energies relative to other comparable batteries (1). Several reviews have explored the current state of the art of these batteries including Lu *et al.* (1) and Kwabi *et al.* (2). Both of these reviews identify several concerns and potential barriers to mass production of Li-air batteries. One of these barriers is identifying the ideal stable electrolyte for maximal Li⁺ transport (1). Electrolyte selection is a daunting experimental task, particularly because countless possible electrolyte materials exist and it is impractical to measure all of their transport

properties. However, models can assist in down selecting potential electrolyte materials by identifying specific characteristics of electrolytes that lead to superior properties. In particular, molecular dynamics (MD) can simulate diffusion with sufficient detail to identify the controlling mechanisms and estimate the associated transport coefficients. Yet, in order for MD models to effectively select optimal materials based on ion transport efficiency, an interatomic potential must accurately reproduce some important material properties, in particular, the density (ρ) and the transition temperature (glass and/or melt, denoted T_t).

We have chosen not to specifically call T_{ta} glass transition or melting temperature for several reasons. While the material investigated in this work has an experimentally defined melting temperature, the techniques discussed here are not typically used for determining melting temperatures. While there is correlation between the temperatures we calculate and the actual melting temperature, we refrain from calling it such. The techniques we do employ are typically used for calculating glass transition temperatures, even though this material does not have a strict transition from a glassy polymer to a rubbery polymer.

Herein we explore the ability of one interatomic potential (18) to reproduce ρ and T_t in some commonly used electrolytes: ethylene carbonate (EC) and propylene carbonate (PC). It is now known that these are not optimal electrolytes for Li-air batteries due to unwanted interactions with the lithium anode (1), but they are excellent materials for exploring modeling methodologies because of the wealth of available data in the literature (3,4,5,6,18). We begin by comparing the results of the original potential parameterization to measured material properties as a point of reference. The potential's long-range van der Waals interactions, between molecules, are then modified to correctly reproduce the ratio of EC to PC T_t 's. The results presented here will describe the steps in determining ρ and T_t followed by a method for modifying the EC interactions of the potential to improve its predicted properties.

Methodology

Many interatomic potentials have been parameterized to model organic compounds including non-reactive MM3 (7,8,9), DREIDING (10), UFF (11) and the more complicated reactive models REBO (12,13,14), AIREBO (15), and REAXFF (16). The CHARMM interatomic potential (17) is similar to the cited non-reactive potentials and includes the long-range contributions from van der Waals and Columbic interactions. For CHARMM the total potential energy (V) is represented as:

$$V = E_{\text{intra}} + E_{\text{inter}} \quad [1]$$

where

$$\begin{aligned} E_{\text{intra}} = & \sum_{\text{bonds}} k_b (b - b_0)^2 + \sum_{\text{angles}} k_\theta (\theta - \theta_0)^2 + \sum_{\text{dihedrals}} k_\phi [1 + \cos(n\phi - \delta)] \\ & + \sum_{\text{impropers}} k_\omega (\omega - \omega_0)^2 \end{aligned} \quad [2]$$

and

$$E_{\text{inter}} = \sum_N \epsilon_{vW} \left[\left(\frac{R_{\min_{i,j}}}{r_{ij}} \right)^{12} - \left(\frac{R_{\min_{i,j}}}{r_{ij}} \right)^6 \right] + \frac{q_i q_j}{\epsilon_q r_{ij}} \quad [3]$$

The total energy includes terms for both intramolecular (E_{intra}) and intermolecular (E_{inter}) interactions. Intramolecular interactions are characterized by bond stiffnesses (k) penalizing deviations from equilibrium bond lengths (b_0), angles (θ_0), dihedral orientations (n, δ), and in-plane improper orientations (ω_0). The intermolecular interactions are given by 12-6 Lennard-Jones (LJ) and Coulombic contributions, where ϵ_{vW} and $R_{\min_{i,j}}$ are the LJ energy and distance constants, respectively, q_i is the point charge for atom i , ϵ_q is the effective dielectric permittivity, and r_{ij} is the distance between atoms i and j . A number of different parameterizations exist for EC and PC (3,5,6,18) which have been used in simulations to explore Li^+ transport properties. In this work, we use the parameterization from SwissParam (18) to provide the initial guess for all parameters.

While the intramolecular terms are important, particularly for large molecules with multiple configurations and conformations, for smaller molecules such as EC and PC they are less relevant for determining transport properties. The intermolecular terms contribute most significantly to thermo-mechanical behavior, namely T_t , of materials comprised of smaller molecules. Since the intramolecular terms do not significantly affect for the targeted material properties they are not modified. A list of all unmodified parameters is given for reference in Appendix A.

Before analysis can begin relaxed, equilibrium structures must be constructed. The (artificial) initial structure is based on a 500 x 500 x 500 close-packed lattice. Each node of the lattice is a possible molecule or ion location. The nearest node distances are chosen to be slightly larger than the largest molecule dimension, PC in this case. The lattice is then populated randomly with a predetermined number of molecules with random orientations. All simulations contain 1,000 molecules. Generally this results in a very low-density material. The initial structure is then run through a series of MD stages to arrive at an equilibrium structure. All MD simulations employ the LAMMPS (19) software package.

The first stage removes high-energy configurations. After initializing velocities from Boltzmann distribution at 300K, constant volume and energy (NVE) dynamics are run with a maximum atom displacement per time step of 0.05 Å for 10 million time steps of 0.05 fs. The next stage uses a Nosé-Hoover thermostat/barostat for constant pressure and temperature dynamics (NPT) (20) to maintain the temperature at 300K and compress the system to a pressure of 2000 bar. This second stage has a duration of 2 million time steps at 0.1 fs. The system is then maintained at 300K and 2000 bar for 5 million time steps at 0.1 fs. Following this stage all of the remaining dynamics use a time step of 0.5 fs. The pressure is then ramped down to 1 bar over 5 million time steps. The system is now at the desired initial thermodynamic conditions for determining physical properties. However, systems consisting of large molecules can often have a large number of initial conformations and the particular configuration is highly dependent on the equilibration history. Thus, in order to fully equilibrate the system it must be cycled through a number

of heating and cooling steps. We use an operational definition of equilibrium: a system equilibrated if it returns to the same volume at a given temperature after a heating and cooling cycle. Typically, two to three cycles are sufficient for T_t to converge. Each cycle begins by heating the sample from 300K to 600K for 5 million time steps. The simulation is then cooled to 100K again over 5 million time steps. Each cycle concludes with reheating the sample from 100K to 300K over 5 million time steps. Furthermore, due to the infinite number of potential initial configurations it is possible for a single configuration to have a spurious response. In order to mitigate this issue, each result is the average of ten different initial configurations all going through the same equilibration process.

To analyze the response of the potential three different initial configurations are considered: 1000 PC molecules (100% PC), 536 EC and 464 PC molecules (50% EC/50% PC by mass), and 1000 EC molecules (100% EC). Once the systems are sufficiently equilibrated, T_t are determined by finding the intersection between the two linear regimes in the volume versus temperature (V-T) curve, similar to Han *et al.* (21). Below T_t the volume does not increase with increasing temperature as drastically as above the transition. While the transition is gradual, extending tangents from the two linear regimes results in a unique intersection and bisection line. The intersection of the the bisection line and the data curve defines T_t . This method of determining T_t is chosen for its algorithmic simplicity. Other methods such as the two-phase equilibrium technique (22) are more applicable to crystalline materials.

Application

Figure 1a shows the V-T response for the original SwissParam parameterization for the three different mixtures. Clearly, there is not a significant difference in the T_t between the three configurations. In fact, if the volumes are normalized by the average volume at 100K for each simulation, simply to make the comparison between systems easier, the curves fall on top of each other, as shown in Figure 1b. All three curves correspond to a T_t of \sim 265K. Figure 1b also shows the tangent lines used to determine T_t . This result is not that surprising, considering the potentials for each molecule are essentially the same outside of slight differences in the electrostatic point charges on each atom (see Figure A1 in Appendix). The only difference between the EC and PC molecules is the additional methyl group on the PC molecule. Thus, the geometric considerations are not sufficient to cause a difference in material response. This has potential impact on assisting material selection. In this case, thermomechanical properties of molecules with similar geometry could solely depend on the strength of intermolecular interactions. A T_t of 265 K for PC is within 18% of the measured melting temperature of 224 K (23) and most importantly is liquid at room temperature (298K). Additionally, the calculated ρ of PC is 1.18 g/cm³, which is again in excellent agreement with the measured value of 1.20 g/cm³ (23). However, a T_t of 265K for EC is far too low because EC is a solid at room temperature with a measured melting temperature of 309 K and ρ of 1.32 g/cm³ (23). Nevertheless, the SwissParam parameterization predicts a reasonable ρ of 1.26 g/cm³.

With a reasonable representation of T_t and ρ of PC, the original parameterization is expected to reproduce the correct behavior at room temperature. However, the EC parameterization does not allow for differentiation between the properties of the two

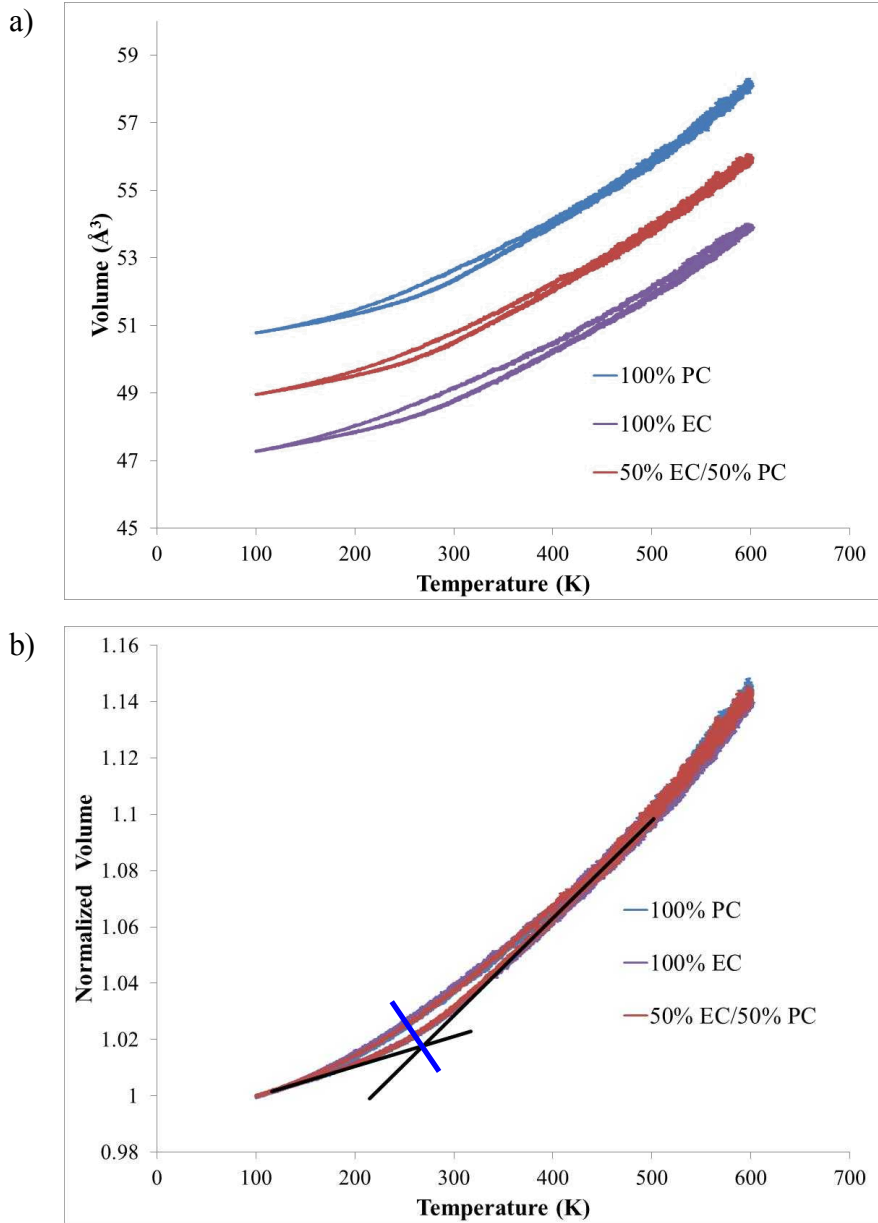


Figure 1: Volume versus temperature curves for the original potential parameterization for 100% PC, 100% EC and 50% EC- 50% PC (by mass) configurations a) Non-normalized volumes; b) volumes, normalized by the 100K volumes. The black tangent lines and blue bisection line illustrate the method for determining the transition temperature.

materials and will result in insufficient predictions of room temperature ion transport properties in pure EC and potentially high EC content mixed electrolytes (90% EC/ 10% PC has a measured melting temperature of 302 K(24)). To resolve this problem, the van der Waals parameter (ϵ_{vW}) magnitudes of EC were systematically increased, strengthening the relative attraction between the molecules. The ϵ_{vW} represents the energy well depth of the LJ pair-potential. Increasing the magnitude of this parameter strengthens the attraction between atoms/molecules. This attraction directly influences the density and relative stability of the material. We considered three different ϵ_{vW}

values, increasing by 100%, 50%, and 25% above the original values. The final V-T cycles of all four EC potentials are shown in Figure 2.

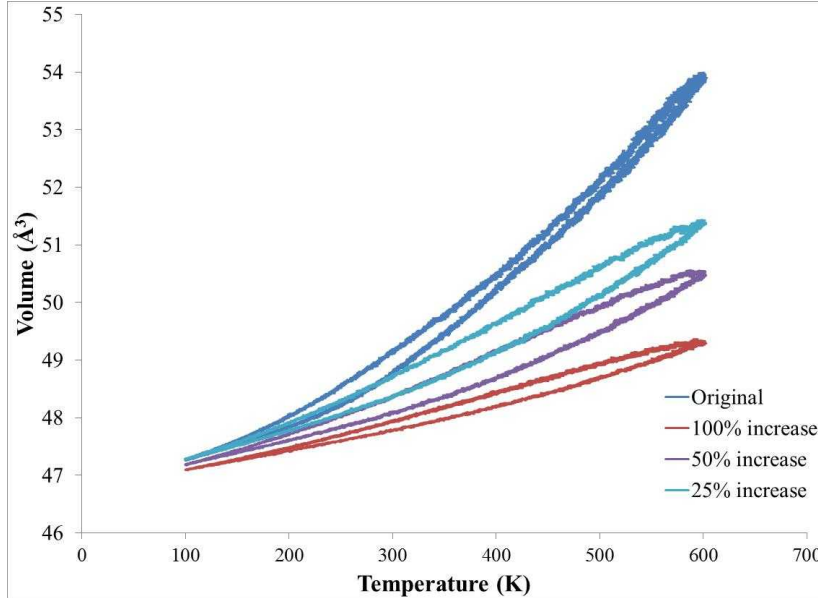


Figure 2: Volume versus temperature curves for four different parameterizations of the ethylene carbonate potential. The interatomic ϵ_{vW} parameter is increased by 100%, 50%, and 25% over the original values.

The ρ and T_t of each parameterization are reported in Table I. Increasing the ϵ_{vW} values effectively strengthens the bonding between molecules causing the material to become denser and increases the T_t .

TABLE I. Densities (ρ) and transition temperatures (T_t) of different interatomic parameterizations of ethylene carbonate

% increase of ϵ_{vW}	ρ (g/cm ³)	T_t (K)
0 original	1.26	265
25	1.29	325
50	1.32	355
100	1.34	385

Each 25% increase in ϵ_{vW} increases the ρ by ~ 0.02 - 0.03 g/cm³ and T_t by anywhere from 30-60 K. The potential matches the experimentally measured ρ of 1.32 g/cm³ by increasing ϵ_{vW} 50%. However, this increases the T_t \sim 50K above the experimentally measured value. An excellent compromise between ρ and T_t is reached if ϵ_{LJ} is increased by 25% of the original values for each of the EC molecules. A comparison of the new and original EC interatomic parameters is listed in Table II.

TABLE II. Comparison of modified potential ϵ_{LJ} with the original SwissParam values (18).

Atom type	Modified EC ϵ_{LJ} (eV)	Original EC and PC ϵ_{LJ} (eV)
C	0.002981	0.002385
O	0.008244	0.006595

C*	0.005963	0.00477
O*	0.006505	0.005204
H	0.001193	0.000954

In addition to changing the interactions between the EC molecules, the interactions of EC molecules with PC and any other entities will also change, since Lorentz-Berthelot combination rules determine the cross element potentials. It is important to note that the intramolecular van der Waals parameters have not been modified, *i.e.*, those dictating interactions beyond the dihedral angle and enumerated in Table A-1. Figure 3 shows the new potential response to the V-T heating cooling cycle. A clear difference now exists between the responses of EC and PC. The new parameterization now predicts an EC T_t of 325K and a ρ of 1.29 g/cm³. The properties of the modified potential are compared to the previous parameterization in Table III. While the T_t for both EC and PC are now higher than the experimental values, the most important aspect to capture is that EC is solid at room temperature while PC is liquid. An added benefit of modifying the EC potential is the increased ρ that comes closer to the experimentally measured value.

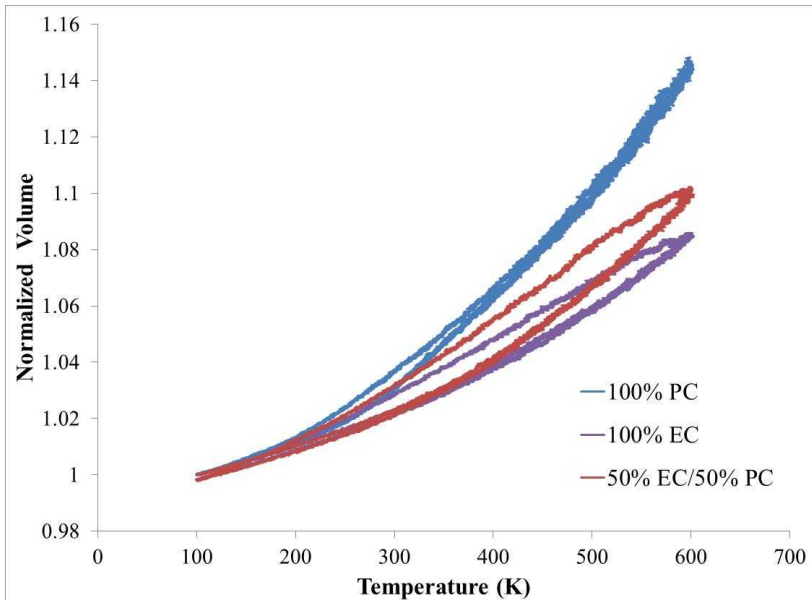


Figure 3: Volumes normalized by the 100K volumes versus temperature for the modified EC potential.

TABLE III. Properties of pure EC, pure PC, and a 50% mixture by mass of EC and PC for the original potential (18), modified potential, and experimental values (^a23 ^b24).

Parameter	Original Potential	Modified Potential	Experimental
EC			
ρ (g/cm ³)	1.26	1.29	1.32 ^a
T_t (K)	265	325	309 ^a
PC			
ρ (g/cm ³)	1.18	1.18	1.20 ^a
T_t (K)	265	265	224 ^a
EC/PC			
ρ (g/cm ³)	1.2	1.24	-
T_t (K)	265	285	271 ^b

Summary

We have presented a modified parameterization for the EC CHARMM potential that captures the difference in T_t relative to PC with the fidelity required to explore Li/Air battery performance at normal operating conditions. While the new parameterization over-predicts the T_t , this potential now accurately predicts solid EC and liquid PC at the temperature of most interest, room temperature. Not only does this parameterization improve the T_t but the simulated ρ of EC is also increased to within 0.03 g/cm³ of the experimental measured value. This new parameterization establishes a method for effectively calculating ion transport properties through arbitrary EC/PC configurations at room temperature. For this case, simply uniformly scaling the van der Waals parameters of an entire molecule produces the desired results. However, the techniques reveal that other parameters can be explored such as ion solvation structure. In contrast to scaling all parameters, adjusting parameters of individual atoms in a molecule would change the orientation of bonding and could lead to tailoring molecules for desired electrolyte properties. This work demonstrates the need for additional effort to develop accurate molecular models of possible Li/Air electrolytes to enable model-guided material selection, which is crucial to explore the complete materials parameter space and identify promising candidates for next-generation batteries.

Acknowledgments

Sandia National Laboratories is a multiprogram laboratory managed and operated by Sandia Corporation, a wholly owned subsidiary of Lockheed Martin Corporation, for the US Department of Energy's National Nuclear Security Administration under contract DE-AC04-94AL85000 (SAND2014-3909 J). Funding for this work was provided by the ASC Verification and Validation program at Sandia, and its support is gratefully acknowledged.

Appendix A: CHARMM PARAMETERS

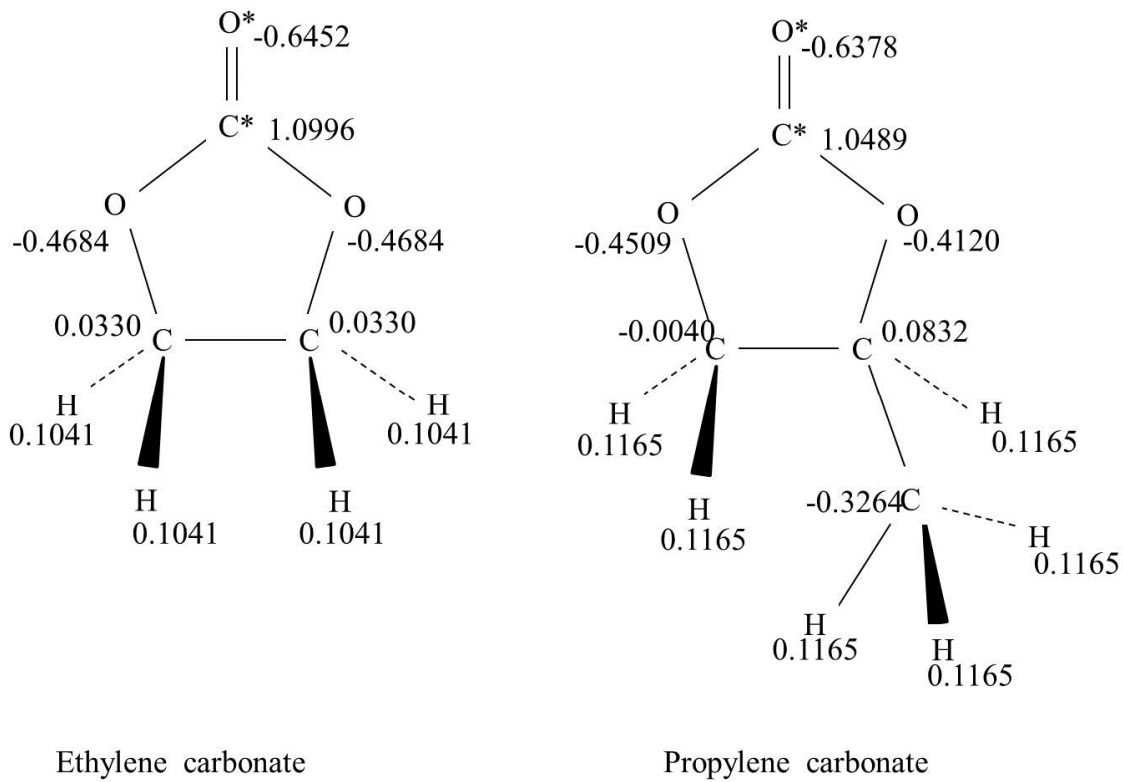


Figure A1: Schematic for ethylene carbonate and propylene carbonate with point charge values.

TABLE A-I. Fixed Potential Parameters from SwissParam (18)

$E_{LJ}(1-4)$	ϵ_{LJ} (eV)	$R_{min,j}$ (Å)
C	0.000434	3.38541
O	0.006595	3.15378
C*	0.004770	3.02905
O*	0.005204	2.49452
H	0.000954	2.35197
E_{bond}	k_b (eV/Å)	b_θ (Å)
C-O	80.82615	1.222
C-C	36.20635	1.355
C-H	31.50039	1.418
O-C*	26.57586	1.508
C*-O*	29.74651	1.093
E_{angle}	k_θ (eV/Å)	θ_θ (Å)
O-C*-O*	7.20875	124.425
O-C*-O	10.47292	109.094
C-O-C*	5.760781	108.055
C-C-O	6.19141	108.133
O-C-H	4.874444	108.577
H-C-H	3.22054	108.836
C-C-H	3.96945	110.549
C-C-C	5.311394	109.608

<i>E_{dihedral}</i>	<i>N</i>	<i>k_φ</i> (eV)	<i>δ</i>
C-O-C*-O*	1	0.014786	0
C-O-C*-O*	2	0.155761	180
C-O-C*-O*	3	-0.02029	0
H-C-O-C*	1	0.012402	0
H-C-O-C*	3	-0.00659	0
C-C-O-C*	1	-0.01188	0
C-C-O-C*	3	0.006938	0
C-C-O-C*	2	0.119249	180
O-C-C-O	1	0.008846	0
O-C-C-O	2	0.030311	180
O-C-C-O	3	0.020814	0
O-C-C-H	1	-0.01418	0
O-C-C-H	2	0.023243	180
O-C-C-H	3	0.006071	0
H-C-C-H	1	0.006157	0
H-C-C-H	2	-0.03005	180
H-C-C-H	3	0.006806	0
C-C-C-O	1	-0.01492	0
C-C-C-O	2	0.38074	180
C-C-C-O	3	0.010321	0
C-C-C-H	1	0.013876	0
C-C-C-H	2	-0.01366	180
C-C-C-H	3	0.005724	0
<i>E_{improper}</i>	<i>k_ω</i>	<i>ω₀</i>	
C-H-C-H	0	0	
C*-O-O-O*	0.811416	0	

References

- ¹ Y.-C. Lu, B.M. Gallant, D.G. Kwabi, J.R. Harding, R. R. Mitchell, M.S. Wittingham, and Y. Shao-Horn, *Energy Environ. Sci.* 6, 750 (2013).
- ² D.G. Kwabi, N. Ortiz-Vitoriano, S.A. Freunberger, Y. Chen, N. Imanishi, P.G. Bruce, and Y. Shao-Horn, *MRS Bulletin*, 39, 443 (2014).
- ³ J.C. Soetens, C. Millot, and B. Maigret, *J. Phys. Chem. A*, 102, 1055 (1998).
- ⁴ H. Tsunekawa, A. Narumi, M. Sano, A. Hiwara, M. Fujita, and H. Yokoyama, *J. Phys. Chem. B* 107, 10962 (2003).
- ⁵ M. Takeuchi, Y. Kameda, Y. Umebayashi, S. Ogawa, T. Sonoda, S.-i. Ishiguro, M. Fugita, and M. Sano, *J. Molec. Liq.*, 148, 99 (2009).
- ⁶ O.O. Postupna, Y. V. Kolesnik, O.N. Kalugin, and O. V. Prezhdo, *J. Phys. Chem. B*, 115, 14563 (2011).
- ⁷ N. L. Allinger, Y. H. Yuh, and J.-H. Lii, *J. Am. Chem. Soc.*, 111, 8551 (1989).
- ⁸ N. L. Allinger, F. Li, and L. Yan, *J. Comput. Chem.*, 11, 848 (1990).
- ⁹ N. L. Allinger, F. Li, L. Yan, and J. Tai, *J. Comut. Chem.* 11, 868 (1990).
- ¹⁰ S. L. Mayo, B. D. Olafson, and W. A. Goddard, *J. Phys. Chem.*, 94, 8897 (1990).
- ¹¹ A. K. Rappé, C. J. Caswit, K. S. Colwell, and W. M. Skiff, *J. Am. Chem. Soc.*, 114, 10024 (1992).
- ¹² D. W. Brenner, *Phys. Rev. B*, 42, 9458 (1990).
- ¹³ D. W. Brenner, *Phys. Rev. B*, 46, 1948 (1992).
- ¹⁴ D. W. Brenner, J. A. Harrison, C. T. White, and R. J. Colton, *Thin Solid Films*, 206, 220 (1991).
- ¹⁵ S. J. Stuart, A. B. Tutein, and J. A. Harrison, *J. Chm. Phys.*, 112, 6472 (2000).
- ¹⁶ A.C.T. van Duin, S. Dasgupta, F. Lorant, and W. A. Goddard III, *J. Phys. Chem. A*, 105, 9396 (2001).
- ¹⁷ B. R. Brooks, R. E. Bruccoleri, B. D. Olafson, D. J. States, S. Swaminathan, and M. J. Karplus, *J. Comput. Chem.*, 4, 187 (1983).

¹⁸ V. Zoete, M. A. Cuendet, A. Grosdidier, and O. Michelin, *J. Comput. Chem.*, 32, 2359 (2011).

¹⁹ S. Plimpton, *J. Comp. Phys.*, 117, 1 (1995).

²⁰ W. Shinoda, M. Shiga, and M. Mikami, *Phys. Rev. B*, 69, 134103 (2004).

²¹ J. Han, R. H. Gee, and R. H. Boyd, *MacroMolecules*, 27, 7781 (1994).

²² J.R. Morris, C.Z. Wang, K.M. Ho, and C.T. Chan, *Phys. Rev. B* 49, 3109 (1994).

²³ CRC Handbook of Chemistry and Physics, W.M. Haynes and D.R. Lide Editors, CRC press, Boca Raton, FL (2011).

²⁴ M.S. Ding, *J. Chem. Eng. Data*, 49, 276 (2004).